Ultrasensitive Bioelectronic Tongue Based on the Venus Flytrap Domain of a Human Sweet Taste Receptor

Jin-Young Jeong, Yeon Kyung Cha, Sae Ryun Ahn, Junghyun Shin, Yoonji Choi, Tai Hyun Park, Seunghun Hong

Ultrasensitive Bioelectronic Tongue Based on Venus Flytrap Domain of Human Sweet Taste Receptor

Jin-Young Jeong[a,†], Yeon Kyung Cha[b,†], Sae Ryun Ahn[c], Junghyun Shin[a], Yoonji Choi[a], Tai Hyun Park[b,d,], and Seunghun Hong[a,*]*

[a]Department of Physics and Astronomy, Seoul National University, Seoul, 08826, Korea

[b]Interdisciplinary Program in Bioengineering, Seoul National University, Seoul, 08826 Korea

[c]Industry Collaboration Center, Industry-Academic Cooperation Foundation, Sookmyung Women's University, Seoul, 04310, Korea

[d]School of Chemical and Biological Engineering, Institute of Chemical Processes, Seoul National University, Seoul, 08826, Korea

[*] To whom correspondence should be addressed.

E-mail: seunghun@snu.ac.kr (S. Hong), thpark@snu.ac.kr (T.H. Park)

ABSTRACT

Sweet taste is an important factor that regulates calorie intake and contributes to food preferences in humans and animals. Therefore, the evaluation of sweet substances is essential for various fields such as healthcare, food, and pharmaceutical industries. Sweet tastants are detected by sweet taste receptors which are class C G-protein-coupled receptors (GPCRs). T1R2 venus flytrap (VFT) of sweet taste receptor is known as a primary ligand-binding domain for sweet tastants. In this study, we developed an ultrasensitive artificial sweet taste bioelectronic tongue based on the T1R2 VFT of a human sweet taste receptor. Here, the T1R2 VFT of a human sweet taste receptor was successfully overexpressed in a bacterial expression system. A T1R2 VFT-immobilized carbon nanotube field-effect transistor with floating electrodes was exploited as an artificial sweet taste sensory system. Significantly, our T1R2 VFT-functionalized bioelectronic tongue could be used to detect solutions of sweet tastants down to 0.1 fM and selectively discriminate sweet substances from other taste substances. Furthermore, our device could be used to monitor the response of T1R2 VFT domain of a sweet taste receptor to sweet substances in real food environments such as apple juice and chamomile herb tea. Moreover, our device was used to evaluate the *inhibition* and *enhancement* effects on sweet taste receptors by *zinc ions* and *chamomile tea*, respectively. In addition, our device demonstrated a long-term storability and reusability. In this respect, our sweet taste bioelectronic tongue could be a promising tool for various basic research and industrial applications.

KEYWORDS

bioelectronic sensor, sweet taste sensor, human sweet taste receptor, G-protein-coupled receptor, venus flytrap, carbon nanotube, field-effect transistor

1. INTRODUCTION

Recognizing sweet substances is essential for the survival of humans and animals in terms of controlling caloric intake and contributing to food preferences.[1, 2] The sense of sweetness comes from carbohydrates, the main energy source of the human diet. Carbohydrates and their derivatives play significant roles in various physiological processes such as energy storage, immune system, fertilization, and cell development.[3-5] However, an excessive carbohydrate intake can cause chronic diseases such as obesity, diabetes, hypertension, and metabolic syndrome.[6-8] Accordingly, as the demand for calorie-free sweeteners is greatly increased, research and development of calorie-free sweeteners and sweetness modulators are attracting attention. Therefore, it is important to evaluate sweet substances in food for various fields such as healthcare, food, and pharmaceutical industries.[9]

Various methods for the detection and evaluation of sweet substances have been developed. Among them, human sensory evaluation is the most commonly used method. However, limitations exist, such as a slow test speed and individual deviation in taste sensitivity.[10] Accordingly, interest in standardization of taste is increasing, and various methods for objective evaluation of sweet substances have been developed. Examples of such methods include high-performance liquid chromatography[11, 12], sensors using lipid polymer membrane[13], electrochemical methods[14, 15], and surface plasmon resonance spectroscopy.[16, 17] Although these techniques have been successfully used to analytically detect sweet substances, they featured low selectivity and could not mimic versatile natural features of the human taste system such as the synergistic effect of sweeteners.[18] In recent years, bioelectronic tongues have been developed to converge the advantages and

overcome the limitations of human sensory evaluation and conventional measurement methods. For example, nanovesicle-based[19, 20] and receptor protein-based[21-23] artificial taste sensors have been developed. The devices showed a human-like performance in detecting taste substances. Also, nanovesicles-based bioelectronic tongues could mimic the natural environment in cells and allowed a fully functional structure of membrane protein. However, it is still challenging due to complicated manufacturing process and low protein expression yield. Receptor protein-based bioelectronic tongues allowed facile fabrication in terms of high-level production of proteins using bacterial expression and showed advantages in stability and reusability.[24] In addition, the receptor protein-based devices demonstrated a lower detection limit than bioelectronic tongues based on receptor-carrying nanovesicles which showed a detection limit of a micro-molar level.[19, 20] However, sweet taste receptor, which is a class C GPCR, is difficult to express in bacterial systems due to its large and complex structure.[25, 26] In a previous study, an effort has been made to utilize only the ligand-binding domain of class C GPCR as a detection element for umami tastants, while it has not been applied to bioelectronic tongue devices for the sensitive detection of sweet tastants.[21]

Herein, we report an ultrasensitive bioelectronic tongue based on a venus flytrap (VFT), the primary ligand-binding domain of a human sweet taste receptor, for the detection of sweet substances. In this strategy, only the T1R2 VFT of a human sweet taste receptor was produced from *Escherichia coli* (*E. coli*). Then, it was immobilized on floating electrodes of a carbon nanotube field-effect transistor (CNT-FET) to build a sensitive bioelectronic tongue device. Our T1R2 VFT-functionalized bioelectronic tongue device could be used to detect sweet substances with a concentration down to 0.1 fM in drink samples such as apple juice and chamomile herb tea. It indicates a 10^7 times higher sensitivity compared with previously-reported sweet taste sensors.[15,

[20, 27, 28] Furthermore, our device was used to evaluate the *inhibitory* and *synergistic* effects of *zinc ions* and *chamomile tea* on sweet taste perception, respectively. Moreover, our sensor exhibited a high stability over a long storage period and could be reused multiple times. In this sense, our T1R2 VFT-based bioelectronic tongue device could be a promising platform for basic research and versatile industrial applications.

2. EXPERIMENTAL SECTION

Materials. Semiconducting single-walled CNTs with a 99% purity were purchased from NanoIngetris (Canada) and used as received. Sucrose, saccharin, $ZnSO_4$, and HEPES buffer were purchased from Sigma-Aldrich (USA). N-hydroxysulfosuccinimide (NHS) and 1-ethyl-3-(3-dimethylaminopropyl)carbodiimide (EDC) were obtained from Thermo Scientific (USA). Commercial beverages of apple juice and chamomile tea were purchased from a grocery store in Korea.

Gene cloning of T1R2 VFT. Signal peptide (1-20 aminoacids)-deleted T1R2 VFT gene was amplified by polymerase chain reaction (PCR) with human genomic DNA as templates using primers (5′ CAC CAG GAG ATA TAC ATA TGG CTG AGA ACT CG 3′, 5′ GAC ATA GGG ATC GTG TTG 3′). The amino acid sequence of T1R2 VFT is provided in the supporting information (Table S1). A human cDNA, pCMV6-ENTRY-hTAS1R2 was purchased from Origene (USA). Amplified PCR product was cloned into pENTR cloning vector with directional TOPO cloning and then cloned to pET-DEST42 expression vector using LR Clonase (all from Invitrogen). T1R2 VFT gene was cloned into pET-DEST 42 bacterial expression vector with 6xHis gene at the C-terminus for purification (Figure S1).

Expression, solubilization, and purification of T1R2 VFT. The cloned pET-DEST42 T1R2 VFT construct was used to transform an *E. coli* Rosetta™ (DE3) strain and the transformed cell were cultured in a LB media with ampicillin (50 μg/mL) at 37°C. At the optical density (OD_{600}) value of 0.5, T1R2 VFT gene expression was induced using 0.5 mM isopropyl β-D-thiogalactoside (IPTG). Cells were incubated for 4 h and were harvested by centrifugation (7000 g, 20 min, 4°C). Pellets were resuspended in phosphate-buffered saline (PBS) containing 2 mM EDTA (pH 8.0) and were lysed by sonication (5 s on/off, 25% amplitude, 5 min). The sample was then collected by centrifugation (12000 g, 30 min, 4°C). The insoluble fraction including T1R2 VFT was solubilized in solubilization buffer (0.1 M Tris-HCl, 20 mM sodium dodecyl sulfate (SDS), 100 mM dithiothreitol (DTT), 1 mM EDTA, pH 8.0) at 30°C overnight. The solubilized sample was centrifuged (12000 g, 30 min, 30°C) and was collected. The sample was dialyzed in dialysis buffer (0.1 M sodium phosphate, 10 mM SDS, pH 8.0) using MEMBRA-CEL® dialysis membrane (Viskase) of 14 kilodaltons molecular weight cut-off (MWCO). After filtering the dialyzed sample with a 0.45 μm bottle top filter (Thermo Fisher Scientific), the sample was loaded to a 5 ml HisTrap affinity column (GE Healthcare) equilibrated with binding buffer (0.1 M sodium phosphate, 10 mM SDS, pH 8.0). The column was then gradually washed with a washing buffer (0.1 M sodium phosphate, 10 mM SDS, pH 7.0). Finally, T1R2 VFT was eluted with elution buffer (0.1 M sodium phosphate, 10 mM SDS, pH 6.0) and was stored at – 80°C for later use.

Refolding of purified T1R2 VFT. Purified T1R2 VFT was diluted to a concentration of 0.5 mg/ml and dialyzed in 4-(2-hydroxyethyl)-1-piperazineethanesulfonic acid (HEPES) buffer I (20 mM HEPES, 10 mM SDS, 0.5 mM EDTA, pH 8.0) with MEMBRA-CEL® dialysis membrane (Viskase) of 14 kilodaltons MWCO at room temperature. The dialysis buffer was then changed to HEPES buffer II (20 mM HEPES, 5 mM SDS, 0.5 mM EDTA, pH 7.5) at room temperature. Then,

the buffer was replaced to HEPES buffer III (20 mM HEPES, 3 mM SDS, 0.5 mM EDTA, pH 7.5) at room temperature. 10 mM of methyl-β-cyclodextrin was added to the dialyzed protein sample and stirred at 4°C overnight. The mixed sample was dialyzed in refolding buffer (20 mM HEPES, 1 mM EDTA, and 150 mM NaCl, pH 7.5) at 4°C.

Total protein assays, protein electrophoresis, and western blot analysis. The concentration of T1R2 VFT was determined with a BCA assay kit (Pierce). Sodium dodecyl sulfate-polyacrylamide gel electrophoresis (SDS-PAGE) and western blot analysis was performed. For SDS-PAGE, protein samples were incubated with a staining solution (Coomassie Blue 0.5 g/L, acetic acid 7%(v/v), methanol 40%(v/v)) for 1 h at room temperature. The stained gel was incubated with a destaining solution I (acetic acid 7%(v/v), methanol 40%(v/v)) for 1 h at room temperature and then incubated with a destaining solution II (acetic acid 7%(v/v), methanol 5%(v/v)) for overnight at room temperature. For western blot, protein samples were mixed with a 2x Laemmli sample buffer added by 2-Mercaptoethanol (Biorad) and boiled for 5 min at 95°C. After loading the samples and protein markers into the gel, SDS-PAGE was performed at 80 V. Protein bands were transferred to a nitrocellulose membrane and the membrane was incubated with a blocking solution (5 wt% skim milk in PBS-T (1X PBS, 0.1 vol% Tween-20)) at room temperature for 1 h. An anti-His mouse antibody (Santa Cruz Biotechnology) was used as a primary antibody and an HRP-conjugated goat anti-mouse IgG antibody (Merck) was used as a secondary antibody. After washing the membrane several times with PBS-T, the protein band of T1R2 VFT was analyzed using TOPview^{TM} ECL Pico Plus Western Substrate (Enzynomics).

Tryptophan fluorescence quenching assay. The ligand-binding function of refolded T1R2 VFT was analyzed by a tryptophan fluorescence quenching assay using an LS 55 Luminescence Spectrometer (Perkin Elmer). The intrinsic tryptophan fluorescence of T1R2

VFT was measured with excitation at 290 nm and emission at 350 nm. The relative fluorescence intensity was calculated with the formula ($\Delta F/F_0$ (%) = [$(F_0 - F)/F_0$] X 100). F_0 and F refer to the fluorescence intensity of T1R2 VFT *before* and *after* the treatment of taste molecules, respectively.

Fabrication of CNT-FETs. CNTs were dispersed in 1,2-dichlorobenzene by applying ultrasonic vibration for 3h. The concentration of the CNT suspension was 10 μg/ml. A photoresist (AZ5214E) pattern was deposited on a SiO_2 substrate via a photolithography process. A CNT solution was dropped on the patterned substrate. The CNTs were selectively adsorbed on bare SiO_2 regions by a dielectrophoresis method (5 Vpp, 300 kHz, 10 s). Floating electrodes (Pd/Au, 10 nm/15 nm) were deposited by a photolithography process and a thermal evaporation method. The length of a CNT channel was 150 μm, and the width of the channel was 100 μm. The floating electrodes had a length of 300 μm and a width of 10 μm.

Immobilization of T1R2 VFT on the floating electrode of a transistor. A CNT-FET device was incubated in an N-acetyl-L-cysteine solution (0.5 M in distilled water) for 12 h at room temperature. The chip was gently rinsed with distilled water. The device was incubated with a mixture of EDC (20 mM in MES buffer) and NHS (40 mM in MES buffer) for 30 min. The chip was gently rinsed with HEPES buffer. Then, 1 μl of T1R2 VFT in a HEPES solution was dropped on the channel region of the sensor. The sensor was incubated for 2 h at room temperature. The prepared chip was stored at 4°C. The chip was washed to remove unbound protein before each measurement.

Substance Preparations. Sucrose and saccharin were dissolved in a HEPES buffer solution. Apple juice and chamomile tea were filtered with a syringe filter (0.2 μm) and serially diluted in

HEPES buffer. $ZnSO_4$ powder was dissolved in a HEPES buffer solution. Sucrose-added chamomile was prepared by dissolving sucrose (100 mg/ml) in diluted chamomile tea.

Electrical Measurements. A T1R2 VFT-immobilized CNT-FET sensor was connected to a semiconductor characterization system (4200-SCS, Keithley). A 9 μl of HEPES buffer solution was placed on the channel region of the sensor. A constant source-drain voltage of 0.1 V was maintained during the electrical measurement. Various sample solutions were consecutively added to the sensor, and source-drain currents were monitored.

3. RESULTS AND DISCUSSION

The schematic illustration of a human sweet taste receptor is shown in Figure 1a. A human sweet taste receptor has been identified as a heterodimer which is composed of two different G-protein coupled receptor subunits.[29, 30] One is taste receptor type 1 member 2 (T1R2), and the other is type 1 member 3 (T1R3).[26, 31] Each subunit comprises a ligand-binding venus flytrap (VFT) domain, a cysteine-rich domain (CRD), and a transmembrane domain (TMD).[32] The VFT of a T1R2 subunit provides binding sites for most sweet substances such as sucrose, glucose, and saccharin.[31, 33, 34]

Figure 1b depicts the schematic diagram of a floating electrode-based bioelectronic tongue using T1R2 VFT. The scanning electron microscopy image of the channel region in the CNT-FET is shown in Figure S2. Floating electrodes and a CNT channel were constructed between the source and drain electrodes. The detailed fabrication process is described in the Experimental section. In brief, T1R2 VFT was overexpressed in an *E. coli* expression system. It is known to be very difficult to express a whole part of sweet taste receptor protein due to its large and complex heterodimeric structure.[25, 35] In this work, we overexpressed only a T1R2 VFT domain part instead of a whole human sweet taste receptor and used the part as a recognition element for our sensor. The floating

electrodes of the device were functionalized with a cysteine linker, and the overexpressed T1R2 VFT was selectively immobilized on floating electrodes of the CNT-FET via an amide bond. The binding of sweet substances to the T1R2 VFT on the floating electrode changes the conductance of the underlying CNT channel, which allowed us to detect sweet substances in real-time. Since we used a T1R2 VFT domain of a human sweet taste receptor, our device is expected to detect sweet substances with a similar behavior as human tongues.

Figure 2a shows the SDS-PAGE gel staining and western blot analysis of purified T1R2 VFT. Detailed procedures for the analysis are presented in the Experimental section, and SDS-PAGE gel staining and western blot analysis results after cell lysis, solubilization, and purification are provided in Figure S3. The gel staining and western blot analysis showed bands at 54 kDa, which corresponds to the molecular weight of T1R2 VFT which was calculated by the online ExPASy bioinformatics tool. These results indicate that T1R2 VFT was successfully overexpressed and purified. Note that it is difficult to express the whole parts of class C GPCR such as a human sweet taste receptor, and, even expressed GPCR often exhibited a poor functionality. It is because of the large size and complex heterodimeric structure of the GPCR.[25, 35] In our works, only the T1R2 VFT domain of a human sweet taste receptor was expressed and used as a recognition element, which should improve the performance and stability of our devices.

The functionality of refolded T1R2 VFT for sucrose was evaluated using a tryptophan fluorescence quenching assay (Figure 2b). Tryptophan residues in proteins exhibit intrinsic fluorescence at emission wavelength around 350 nm. The fluorescence intensity can be quenched by conformational changes of the proteins as ligands bind to the receptor protein.[36, 37] In this work, the stimulation of T1R2 VFT by sweet substances induced conformational changes of the protein, which lead to the fluorescence quenching of tryptophan residues. As sucrose concentration

increased, the change of relative fluorescence intensity also increased. Similar changes in relative fluorescence intensities were also observed in fructose, glucose, aspartame, and saccharin solutions (Figure S4). The results indicate that the T1R2 VFT was functionally refolded.

Figure 2c is the tryptophan fluorescence quenching assay results using various taste molecules. The 1 μM addition of sucrose, fructose, glucose, aspartame, and saccharin changed fluorescence intensities by 12 - 15%. On the other hand, relative fluorescence intensity changes were less than 3% when sodium cyclamate (cyclamate, artificial sweetener), cellobiose (tasteless disaccharide), monosodium glutamate (MSG, umami tastant), and denatonium benzoate (denatonium, bitter tastant) were introduced. Note that no significant fluorescence change was detected by using cyclamate which is an artificial sweetener known to interact with the transmembrane domain of T1R3.[31] The results indicate that the produced T1R2 VFT can selectively recognize sweet substances.[31, 38]

Figure 2d shows the atomic force microscopy (AFM) topography images of floating electrodes before and after the functionalization of T1R2 VFT. Multiple spots were observed on the T1R2 VFT-immobilized gold electrode, while a clean surface was observed on the bare electrode. The size of the spots is estimated as 12.6 ± 8.1 nm, which is consistent with the size of T1R2 VFT in previous literature.[35] The results indicate the successful immobilization of T1R2 VFT on our device surface.

The real-time response of our T1R2 VFT-immobilized device to various concentrations of sucrose was measured (Figure 3a). Here, the source-drain current of a sensor was monitored in real-time while target sucrose solutions were introduced to the sensor. A constant bias voltage of 0.1 V was maintained during the measurements. Our sensor showed immediate decreases in current by the introduction of sucrose solutions. After some time, the current level was stabilized

at a fixed value. The device usually exhibit a similar behavior when a continuous flow of solution with constant target concentrations was introduced. Importantly, the sensor began to show a response to the introduction of a 0.1 fM sucrose solution. However, a bare device without T1R2 VFT did not show any significant changes (Figure S5), indicating that the response of our device was originated from the binding of sucrose molecule to T1R2 VFT. Note that the result indicates a ~10^7 times improved detection limit compared to previously-reported sensors including bioelectronic nose devices based on a whole receptor molecule.[19, 20, 27, 28] Such a high sensitivity can be attributed to the small size of T1R2 VFT receptor parts used in our device. Presumably, as small VFT domains can exist within the Debye length from the sensor surface, any electrical changes induced by the binding of sweet substances to the T1R2 VFT can more easily affect the conductance of the underlying CNT channels. It also should be mentioned that, due to the device-to-device variation, the initial current level (I_0) of our devices without target molecules can vary, resulting in different current changes (ΔI) by target molecules. In this case, normalized current values ($\Delta I/I_0$) were often utilized as a sensor signal for a reliable measurement in practical applications. Previous works showed that since there is a linear correlation between absolute sensor response (ΔI) and gate dependence ($\mathrm{d}I/\mathrm{d}Vg$), it is possible to compensate device-to-device variation with such a calibration.[39, 40]

Figure 3b illustrates the sensing mechanism of our T1R2 VFT-based bioelectronic tongue. The binding of sweet substances can cause conformational changes in the T1R2 VFT on the floating electrode of the sensor and facilitate a charge redistribution in the protein. Such charge redistribution in T1R2 VFT changes the work function (ϕ_M) of floating electrodes, which modulates a Schottky barrier height (ϕ_{SB}) between the CNT channel and the floating electrode.[41, 42] The increased Schottky barrier acts as an enhanced potential barrier to hole carriers, leading to

a decrease in the CNT channel current. Consequently, the binding of sweet substances to T1R2 VFT causes a current change in our device, allowing us to detect sweet substances in real-time. On the other hand, since some electrodes are exposed to the target solution, there can be a direct electrochemical current by the downstream molecules between the solution and the electrodes. However, when we tested the device *without any CNT channels*, the current levels were, at least, two orders of magnitude lower than those with CNT channels. Thus, we can expect that the effect of such currents is negligible. It is also worth mentioning that although the sweet taste receptor exists as a dimer composed of T1R2 and T1R3, it has been reported that T1R2 VFT is the primary ligand binding site for most sweeteners and ligand binding on the T1R2 VFT initiate a conformation transition, which activates the receptor and results in the signal transduction.[31, 43-45] In addition, the binding characteristics of sweeteners to the VFT domain are consistent with studies using full heterodimeric receptor (T1R2/T1R3).[35, 46]

Normalized signals of our devices to sucrose and saccharin solutions with concentrations from 0.1 fM to 1 μM (Figure 3c). Sucrose is a natural sugar, while saccharin is an artificial sweetener. We repeated the sensing measurements for three devices to obtain mean values and error bars. The normalized signals were obtained by normalizing the current changes with respect to their maximum values. Our device responded to sucrose and saccharin solutions from the concentration of ~0.1 fM, and the response was saturated at around ~1 μM. These results indicate that our sensor could detect sweet substances with a high sensitivity. The response curves were further analyzed by using the Hill equation.[47, 48] The normalized signal N of a device can be written by the Hill equation like

$$N = \frac{C^n}{K_d^n + C^n} \quad (1)$$

where *C, n,* and K_d are *the concentration of sweet tastants*, *a Hill's coefficient*, and *a dissociation constant* for the binding of the tastants to T1R2 VFT, respectively. By fitting the graph, the dissociation constants of *sucrose* and *saccharin* to T1R2 VFT were estimated as 2.05×10^{-11} *M* (7.02×10^{-9} *g/L)* and 6.88×10^{-12} *M* (1.26×10^{-9} *g/L)*, respectively. It indicates that there was only a 3-fold difference in potency values between saccharin and sucrose in our experiment. It should be noted that, in cell-based measurements, the potency of saccharin was much higher than that of sucrose.[49] Such a difference in the measured potency can be attributed to the cellular signaling process. Although sweet taste is almost exclusively transduced by T1R2/T1R3 receptor, the specific amino acid residues which bind to different sweet substances in the T1R2 VFT cleft regions may vary.[44, 50, 51] In addition, the signaling pathways in taste bud cells of caloric and non-caloric sweeteners are different.[52, 53] On the other hand, our experiment measured the direct binding between sweet taste molecules and receptors without relying on a cellular signaling pathway. Thus, our measured potency can be inconsistent with those measured by cellular experiments. Note that when the potency was measured by tryptophan quenching assay, sucrose and saccharin also exhibited a rather small difference in the potency values, which is consistent with our results (Figure 2b and S4). Thus, our results show a meaningful value for the binding of sweet substances to the binding domains in sweet taste receptors. We also measured the sensor responses to sucralose which has a similar chemical structure to sucrose but exhibited much higher potency in cellular experiments (Figure S6). The measured dissociation constant of sucralose is 2.98×10^{-11} M, which is similar to that of sucrose. Note that sucralose and sucrose have similar structures. In addition, the amino acid residues responsible for binding in the T1R2 VFT domain of sucrose and sucralose are known to be quite similar.[51] In this case, the similar dissociation constants of sucralose and sucrose in our experiments can be attributed to the structural similarity of the two

saccharides. However, it should be mentioned that the tendency is somewhat different from the sweetness potency level results measured by other methods such as a human sensory evaluation.[54] Presumably, it is because our method measures only the binding characteristics of sweet taste receptors, while the responses of human tongues are determined by taste signal transmissions at a cellular level as well as receptor characteristics. Further investigation is needed to elucidate with regard to this issue. It also should be discussed that the estimated dissociation constants are much smaller than previously-reported values measured by cell-based fluorescence assays.[29, 49] Presumably, it is because our sensor could directly measure the conformational change of T1R2 VFT, while previous cell-based assays had to go through complex biological signaling processes in the cells to obtain sensing signals. Similar trends were reported in previous studies using other receptor proteins.[47] These results imply that our sensor could detect sweet tastants at much lower concentrations than cell-based assays. However, it also shows that since our sensor measures the binding of sweeteners to the VFT domain unlike the real taste cell environment in which the taste signal is transmitted through a complex signaling process, their response in some cases can be somewhat different from those of the human tongue.

Moreover, the real-time response of our sensor to different taste substances was evaluated (Figure 3d). During the measurements, a constant bias voltage of 0.1 V was maintained. The source-drain currents were monitored while consecutively adding the 1 μM solutions of cellobiose, MSG, and 1 nM solution of sucrose to the sensor. Cellobiose is a tasteless sugar, and MSG is an umami taste substance. The addition of cellobiose and MSG solutions with a rather high concentration caused negligible conductance changes, while 1 nM sucrose solution caused a significant decrease in the conductance of the device. Such a selective response of our sensor can be attributed to the highly-selective binding activity of a T1R2 VFT domain for sweet substances.[31,

[33, 34] The results indicate that our sensor could discriminate sweet substances from other tastants with a high selectivity just like a human tongue.

We also utilized our devices to examine the inhibition effect of zinc ions on sweet taste perception. Figure 4a shows the dose-dependent response curves of our devices to sucrose solutions with or without $ZnSO_4$. We repeated sensing measurements using three devices for each data point to obtain averaged values and error bars. The normalized signals were obtained by normalizing sensor signals with respect to their maximum values. Note that the response curves were shifted toward higher concentration regions in the presence of $ZnSO_4$. We also confirmed that $ZnSO_4$ solution did not directly affect a conductance of a bare CNT-FET without T1R2 VFT (Figure S7). These results indicate that zinc ions work as an inhibitor to T1R2 VFT, and our device responded only to a high concentration sucrose solution with zinc ions as reported previously.[55] By fitting the graph using the Hill equation, we could calculate half-maximal effective concentration (EC_{50}) values with or without $ZnSO_4$. The EC_{50} values were estimated as 2.79×10^{-11}, 1.59×10^{-9}, and 8.30×10^{-6} M with *0 M*, *1 mM*, and *40 mM* $ZnSO_4$ solutions, respectively. The results clearly show that $ZnSO_4$ solutions contribute significantly to the inhibition of the T1R2 VFT responses to sweet substances, which is consistent with previously reported human sensory tests.[55, 56] It should be mentioned that the inhibitory effect in our device is limited to the VFT domain, and thus further studies on the other domains of a human sweet taste receptor are needed. Since our device can directly detect the T1R2 VFT activities without relying on complex biological signaling processes, it can be a promising tool to quantitatively evaluate the effect of various drugs on the activities of receptor proteins.

To show the applicability of our bioelectronic tongues to real samples, we demonstrated the detection of sweet substances in commercial juice and tea. Figures 4b shows the normalized dose-

dependent responses of our devices to diluted apple juice. Detailed procedures are presented in the Experimental section. In brief, commercial apple juice was diluted serially in a HEPES buffer solution. The commercial apple juice used in this experiment contains various natural sweet substances such as sucrose, glucose, and fructose at a total concentration of ~100 mg/ml.[57] For sensing measurements, the conductance changes of our devices were measured while adding various concentrations of diluted apple juice to our devices. The measured sensor signals were normalized with respect to their maximum values to obtain the normalized signals. The device began to exhibit responses from the diluted concentration of 10^{-16} (v/v) and the responses were saturated at around 10^{-4} (v/v). On the other hand, a CNT-based sensor transducer without T1R2 VFT did not respond to the addition of apple juice (Figure S8). The result indicates that the binding of T1R2 VFT and sweet substances in apple juice induced responses in our device. By fitting the data using the Hill equation[58], we could calculate the half-maximal effective concentration (EC_{50}) values of our device. The volume concentration corresponding to EC_{50} value was estimated as 1.00 X 10^{-10} (v/v). Using the known saccharide concentrations in the apple juice, the measured EC_{50} value by a volume ratio can be converted to a mass concentration of 1.00 X 10^{-8} g/L, which is similar to the value for the responses of our sensors to sucrose in figure 3c. These results show that our device can detect a trace amount of sweet substances in complex environments such as apple juice and can be used for the evaluation of commercial beverages.

Figure 4c shows the normalized responses of our device to chamomile tea with different concentrations of sucrose. Detailed methods were shown in the Experimental section. In brief, sucrose was mixed with chamomile tea at a concentration of 100 mg/ml. The tea was diluted serially to obtain solutions with different concentrations. The conductance changes of the devices were monitored as a sensor signal while adding various concentrations of chamomile tea with

sucrose. The sensing signals increased as the concentration of chamomile tea increased. However, the sensor did not respond to the addition of chamomile tea without sucrose (Figure S9). The results indicate that our T1R2 VFT-based sensor can detect sucrose in chamomile tea. By fitting the data using the Hill equation and considering a known sucrose concentration in the tea, we could estimate the EC_{50} value for sucrose in chamomile tea as 1.89 X 10^{-8} g/L, which is similar to the values in a buffer solution and apple juice.

For evaluating the effect of tea on the T1R2 VFT binding activity, we compared our sensor responses to chamomile tea, sucrose solution, and sucrose-added chamomile tea (Figure 4d). Here, chamomile tea was diluted at 1:1000 in a HEPES buffer solution. Sucrose solution was prepared at a concentration of 0.3 mM in a HEPES buffer solution. Sucrose-added chamomile tea was prepared by adding sucrose in diluted chamomile tea to a concentration of 0.3 mM. Sensor responses to sample solutions were quantified using the absolute values of relative conductance change $|\Delta G/G_0|$, where G_0 and ΔG represent *the device conductance before the injection of target solutions* and *the conductance change after the addition of target solutions*, respectively. Note that chamomile tea caused a negligible change of relative conductance, while a sucrose solution caused a 5.9% change. On the other hand, sucrose-added chamomile tea induced a much larger change of 21% to the device than a sucrose solution. These results indicate that chamomile tea enhanced the sensor responses to sucrose significantly. Similar results were observed in tryptophan fluorescence quenching assays (Figure S10). Sucrose-added chamomile tea induced a much larger change in the relative fluorescence intensity than that of the addition of chamomile tea or sucrose solution. Chamomile tea is known to contain various components such as amino acids, minerals, and polyphenols, which may affect the perception of sweetness.[59-61] For example, previous reports show that some amino acids in tea can enhance sweet taste.[62, 63] A further identification of

particular compounds enhancing a sweet sensation is needed and is under investigation. It is also worth mentioning that there are sweet taste substances and enhancers acting on the transmembrane domain, and thus the enhancement effect on the whole sweet taste receptor needs further study. Subsequently, recalibration of the sensor responses after considering the effect of certain compounds in real beverages may be needed for practical applications of our sensors. On the other hand, since our device is based on the VFT domain of human receptor protein, it can be utilized to evaluate the responses of a sweet taste receptor to sweet substances in versatile environments.

We evaluated the stability of our sensor responses after a long-term storage (Figure 5a). Here, multiple sensor chips were fabricated and stored at 4°C for different time periods. Then, each sensor chip was taken out, and its relative conductance changes by the addition of 1 mM sucrose solutions were measured as a sensor signal at room temperature. For each data point, we repeated the measurements with five sensor chips to obtain averaged values and error bars. The sensor signals remained almost the same for up to 7 days. After then, signals gradually decreased as the storage time increased. Note that the normalized sensor signals remained ~5% even after 28 days of storage. It indicates a high stability of our devices over a rather long period. Presumably, since only a part of sweet taste receptor protein was used in our sensor, we can expect a rather high stability compared with those based on whole receptor molecules in nanovesicle-based sensors.

We also tested the reusability of our sensor chips (Figure 5b). Here, a single sensor chip was used repeatedly to detect 1 mM of sucrose solutions for 3 times. After each sensing experiment, the used chip was gently washed 3 times with a HEPES buffer solution and stored in a refrigerator until the following measurement. Sensor signals were normalized with respect to the first measurement signal of each device. We performed the repeated sensing measurements for three sensor chips and obtained the average values and error bars for each data. Note that, in the second

measurement using a single sensor chip, the sensor signals decreased rather dramatically down to about 70% of the first measurement result. However, after then, the sensor exhibited similar responses up to five repeated sensing measurements. The result indicates that, although the sensor performance degraded after the first applications, the sensor, after some calibrations, can still be used to measure sweet substances repeatedly up to five sensing measurements. In the previous study of a T1R1 VFT-based biosensor for umami taste detection, the normalized signal intensity gradually decreased each time it was reused, which is considered as the destruction of the protein-graphene hybrid structure.[21] The relatively high reusability of our T1R2 VFT-based bioelectronic tongue comes from the immobilization of T1R2 VFT via a thiol-gold interaction. Note that previous bioelectronic sensors for sweet tastes were based on nanovesicles with whole receptor molecules.[20] Such nanovesicle-based bioelectronic sensor devices cannot be used repeatedly because the binding of taste molecules to receptors changed the ion concentration in the nanovesicles, which cannot be returned to the initial level.[19, 64] On the other hand, since the binding of sweet substances to T1R2 VFT is reversible, our T1R2 VFT-based sensor could be used repeatedly for multiple sensing operations, which may be important for practical applications in the future. Note that the binding of receptor and ligand is explained by the Langmuir isotherm theory.[58] In solution, a ligand molecule approaches through diffusion and binds to a receptor molecule. Conversely, the bound ligand can break the binding via thermal energies after some time period. It has been reported that class C GPCRs have a VFT domain that vibrates between an open state without ligand and a closed state with ligand.[65] Such reversible binding properties of these receptors enable the reuse of such sensors based on the receptors, which has been reported in several previous studies.[21, 66]

4. CONCLUSIONS

An ultrasensitive sweet taste detection sensory system was successfully developed using a CNT-FET and the T1R2 VFT of a human sweet taste receptor. In this work, only a T1R2 VFT of human sweet taste receptor was overexpressed in a bacterial expression system instead of the whole receptor, and it was combined with a floating-electrode-based CNT-FET device to build an ultrasensitive bioelectronic tongue device for sweet substances. Our device could sensitively detect sweet tastants down to a 0.1 femtomolar level with a high selectivity. Moreover, our sensor could detect sweet substances in commercial beverages such as apple juice and chamomile tea. Our bioelectronic tongue measured the functional modulation of a human sweet receptor by enhancers and inhibitors. However, since our device is only relevant for the VFT domain of a human sweet taste receptor, further study on the function of the other domains of the receptor is needed. It also should be mentioned that since the human tongue relies on the signal transmission at a cellular level as well as receptor responses, our sensor responses in some cases can be somewhat different from those of the human tongue. Furthermore, our devices could be stored over a rather long period of time and used repeatedly. Our sweet taste detection system can be a powerful tool for the detection of sweet substances and has a significant potential for various applications in food industry and basic research.

ASSOCIATED CONTENT

Supporting Information

Amino acid sequence of T1R2 VFT; expression vector containing T1R2 VFT gene; SEM images of CNT-FET; production of T1R2 VFT in E. coli; dose-dependent test results of T1R2 VFT using tryptophan fluorescence quenching assay; real-time responses of bare devices for sucrose, normalized signal to sucralose; ZnSO4, and apple juice; real-time response of the sensor to chamomile tea; tryptophan fluorescence quenching assay

AUTHOR INFORMATION

Corresponding Authors

Tai Hyun Park - School of Chemical and Biological Engineering, Institute of Chemical Processes, Seoul National University, Seoul, 08826, Korea; Email: thpark@snu.ac.kr

Seunghun Hong - Department of Physics and Astronomy, Seoul National University, Seoul, 08826, Korea; Email: seunghun@snu.ac.kr

Authors

Jin-Young Jeong - Department of Physics and Astronomy, Seoul National University, Seoul, 08826, Korea

Yeon Kyung Cha - Interdisciplinary Program in Bioengineering, Seoul National University, Seoul, 08826 Korea

Sae Ryun Ahn - Industry Collaboration Center, Industry-Academic Cooperation Foundation, Sookmyung Women's University, Seoul, 04310, Korea

Junghyun Shin - Department of Physics and Astronomy, Seoul National University, Seoul, 08826, Korea

Yoonji Choi - Department of Physics and Astronomy, Seoul National University, Seoul, 08826, Korea

Author Contributions

[†]J.-Y.J. and Y.K.C. contributed equally to this work. The manuscript was written through contributions of all authors. All authors have given approval to the final version of the manuscript.

Notes

The authors declare no competing financial interest.

ACKNOWLEDGMENT

This work was supported by the National Research Foundation of Korea (NRF) funded by the Ministry of Science and ICT (MSIT) of Korea (No. 2013M3A6B2078961 and 2020R1A2B5B02002152). S. H. would like to acknowledge the support from the Ministry of Trade, Industry & Energy (MOTIE, Korea) (No. 20012390), Samsung Electronics Co. Ltd. (No. 201209-07908-01), and the European Research Council (ERC) under the European Union's Horizon 2020 programme (grant agreement no. 682286). T. H. P. would like to acknowledge the support from the National Research Foundation, funded by the Korea government (MSIP) (NRF-2018R1A2B3004498) and KIST Institutional Program (Project No. 2E30140).

FIGURES

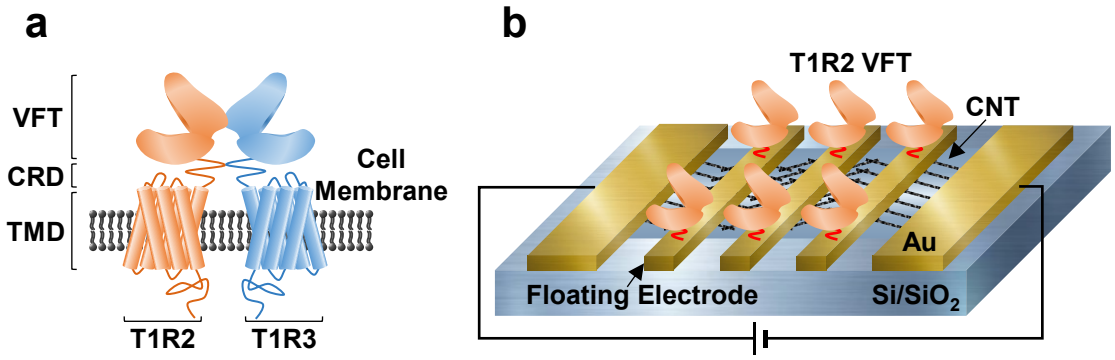

Figure 1. Schematic diagram of a bioelectronic tongue based on T1R2 VFT for the detection of sweet taste substances. (a) Illustration of a human sweet taste receptor. The sweet taste receptor is a heterodimeric complex of T1R2 and T1R3. (b) Schematic diagram of a T1R2 VFT-based bioelectronic tongue for the detection of sweet substances. T1R2 VFT was immobilized on the gold floating electrodes of the CNT-FET using a cysteine linker.

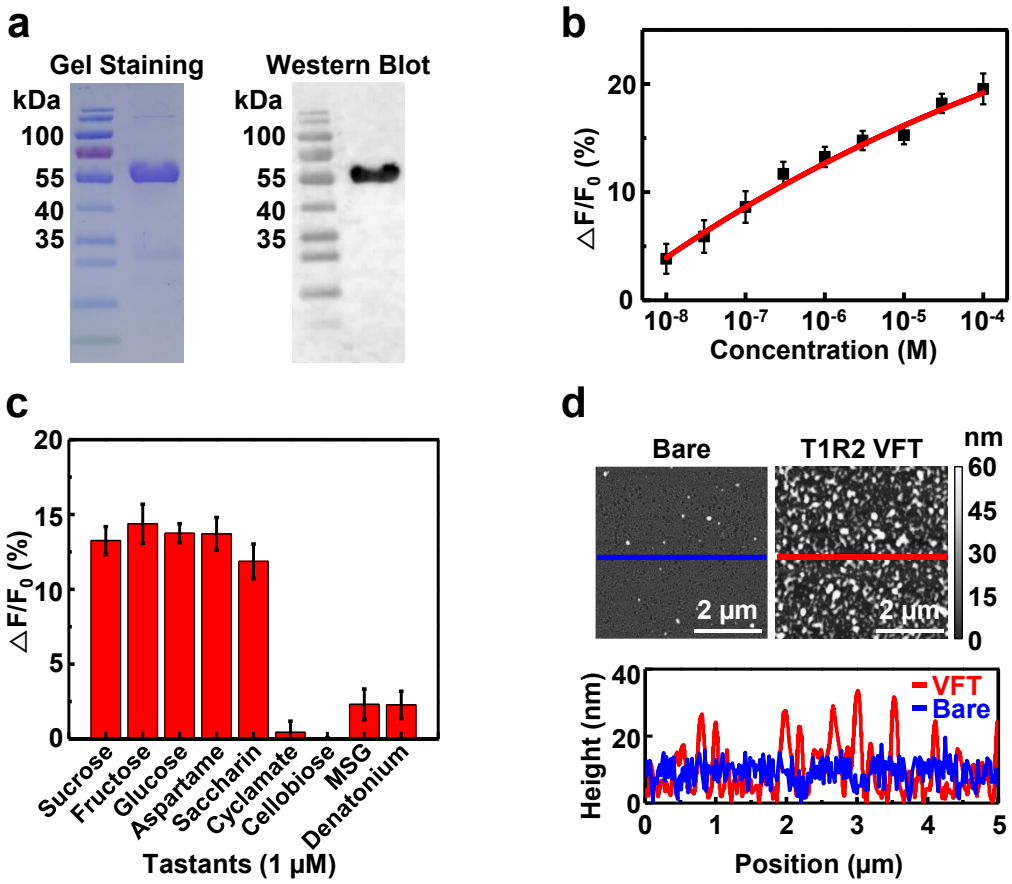

Figure 2. Characterization of T1R2 VFT produced in *E. coli.* (a) SDS-PAGE gel staining (left) and western blot analysis (right) of T1R2 VFT. (b) Dose-dependent tryptophan fluorescence quenching assay results showing the response of T1R2 VFT to sucrose. (c) Selectivity tests of T1R2 VFT with different taste substances using the tryptophan fluorescence quenching assay. Data are expressed as means ± standard deviation (n = 5). (d) AFM images (top) and height profiles (bottom) of floating electrode surfaces before (Bare, blue) and after (T1R2 VFT, red) the immobilization of VFT.

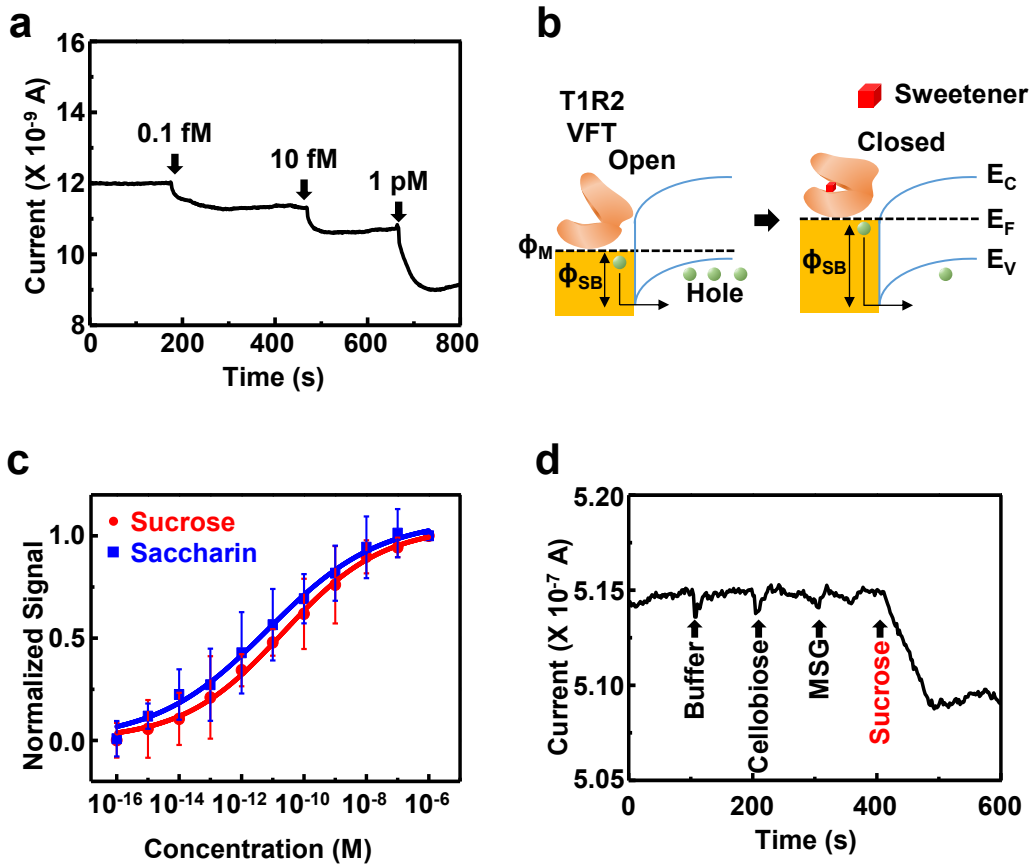

Figure 3. Responses of T1R2 VFT-based bioelectronic tongues to sweet taste substances. (a) Real-time response of a device by the addition of sucrose solutions. The introduction of sucrose solutions caused the decrease of electrical currents. (b) Schematic diagram showing the sensing mechanism of T1R2 VFT-based sensors. T1R2 VFT was immobilized on a floating electrode surface. The energy-band diagram of the floating electrode-based CNT-FET device was depicted below. When the target sweet substance bound to T1R2 VFT, the work function of the floating electrode (ϕ_M) was decreased, which increased Schottky barrier height (ϕ_{SB}). Due to the increased Schottky barrier height, the hole-carrier (green) currents were decreased. E_C, E_F, and E_V represent the *conduction band*, *Fermi-level*, and *valence band* of the CNT channel, respectively. (c) Normalized sensor signals to various concentrations of sucrose (natural sugar) and saccharin

(artificial sweetener). Our device began to show responses to 0.1 fM of sucrose and saccharin, and the signals were saturated at around 1μM. Data are expressed as means ± standard deviation (n = 3). (d) Selective response of the sensor to non-sweet tastants (1 uM of buffer, cellobiose, and MSG) and sucrose (1 nM).

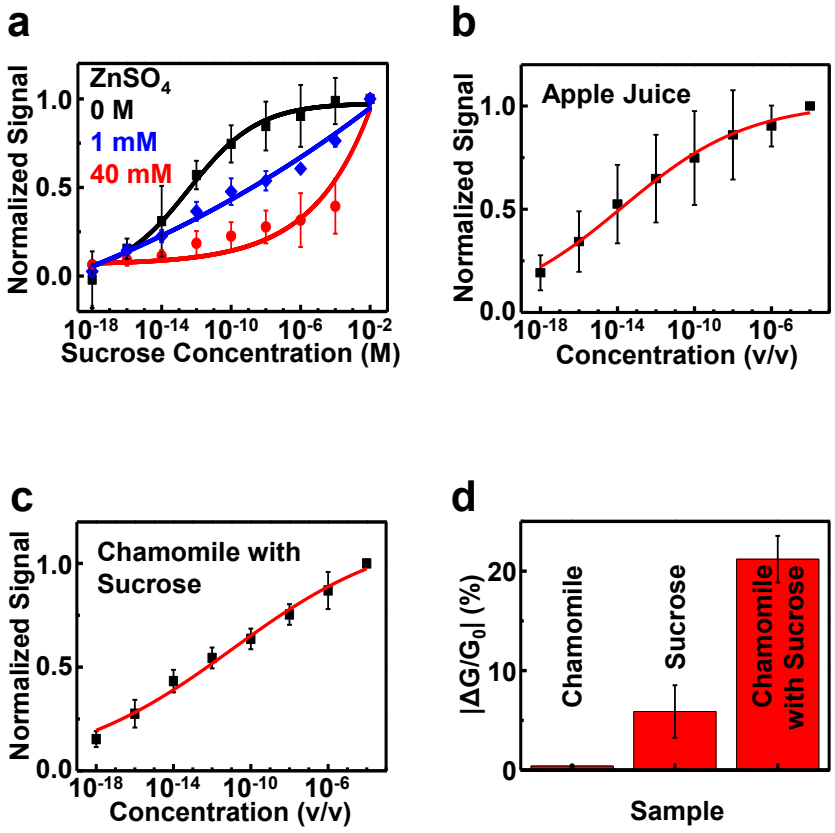

Figure 4. Responses of T1R2 VFT-based bioelectronic tongues in the presence of different chemical species. (a) Dose-response curves of our bioelectronic tongues to sucrose with or without $ZnSO_4$. Zinc ions are known to work as an inhibitor to the binding activities of a human sweet taste receptor. (b) Responses of our bioelectronic tongues to sweet substances in commercial apple juice. (c) Responses to sucrose in chamomile tea. The x-axis represents the volume/volume ratio of the diluted samples in a buffer solution. (d) Relative conductance change of our bioelectronic tongue device by the addition of sucrose with or without chamomile tea. It shows the enhancement of sweet taste by chamomile tea.

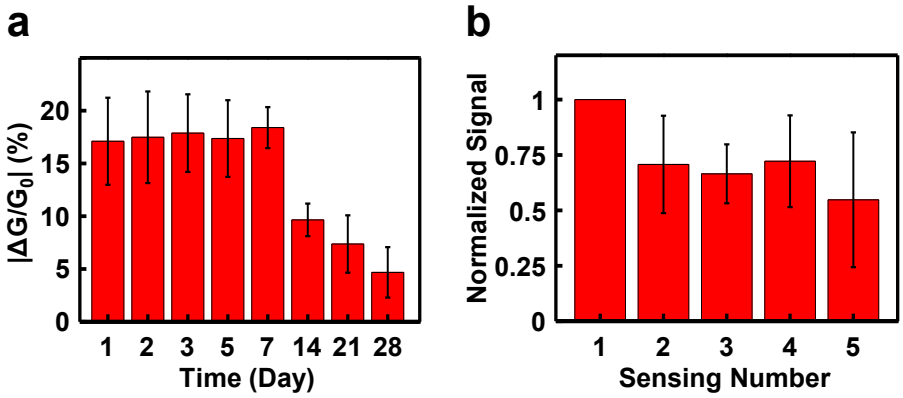

Figure 5. Stability of our bioelectronic tongues. (a) Sensor responses to sucrose after the storage of the sensor chips over a long period up to 28 days. Each *point* and *error bar* indicates the *average value* and *standard deviation*, respectively (n=5). (b) Sensor signals after repeated applications of a single sensor chip. For each data point, the sensing measurement was repeated using three devices to obtain mean values and standard deviations.

REFERENCES

1. Beauchamp, G. K., Why Do We Like Sweet Taste: A Bitter Tale? *Physiol. Behav.* **2016,** *164* (Pt B), 432-437.
2. Ramirez, I., Why Do Sugars Taste Good? *Neurosci. Biobehav. Rev.* **1990,** *14* (2), 125-134.
3. Tecle, E.; Gagneux, P., Sugar-Coated Sperm: Unraveling the Functions of the Mammalian Sperm Glycocalyx. *Mol. Reprod. Dev.* **2015,** *82* (9), 635-650.
4. Ohtsubo, K.; Marth, J. D., Glycosylation in Cellular Mechanisms of Health and Disease. *Cell* **2006,** *126* (5), 855-867.
5. Dwek, R. A., Glycobiology: Toward Understanding the Function of Sugars. *Chem. Rev.* **1996,** *96* (2), 683-720.
6. Mann, J., Dietary Carbohydrate: Relationship to Cardiovascular Disease and Disorders of Carbohydrate Metabolism. *Eur. J. Clin. Nutr.* **2007,** *61* (Suppl 1), S100-111.
7. Mozaffarian, D., Dietary and Policy Priorities for Cardiovascular Disease, Diabetes, and Obesity: A Comprehensive Review. *Circulation* **2016,** *133* (2), 187-225.
8. Ludwig, D. S., The Glycemic Index: Physiological Mechanisms Relating to Obesity, Diabetes, and Cardiovascular Disease. *J. Am. Med. Assoc.* **2002,** *287* (18), 2414-2423.
9. Tahara, Y.; Toko, K., Electronic Tongues–A Review. *IEEE Sensors Journal* **2013,** *13* (8), 3001-3011.
10. Trumbo, P. R.; Appleton, K. M.; de Graaf, K.; Hayes, J. E.; Baer, D. J.; Beauchamp, G. K.; Dwyer, J. T.; Fernstrom, J. D.; Klurfeld, D. M.; Mattes, R. D.; Wise, P. M., Measuring Sweetness in Foods, Beverages, and Diets: Toward Understanding the Role of Sweetness in Health. *Adv. Nutr.* **2021,** *12* (2), 343-354.
11. D'Arcy-Moskwa, E.; Weston, L.; Noble, G. N.; Raidal, S. L., Determination of Sucrose in Equine Serum Using Liquid Chromatography-Mass Spectrometry (LC/MS). *J. Chromatogr. B Analyt. Technol. Biomed. Life Sci.* **2011,** *879* (30), 3668-3671.
12. Terol, A.; Paredes, E.; Maestre, S. E.; Prats, S.; Todoli, J. L., Rapid and Sensitive Determination of Carbohydrates in Foods Using High Temperature Liquid Chromatography with Evaporative Light Scattering Detection. *J. Sep. Sci.* **2012,** *35* (8), 929-936.
13. Habara, M.; Ikezaki, H.; Toko, K., Study of Sweet Taste Evaluation Using Taste Sensor with Lipid/Polymer Membranes. *Biosens. Bioelectron.* **2004,** *19* (12), 1559-1563.
14. Arrieta, A. A.; Apetrei, C.; Rodríguez-Méndez, M. L.; de Saja, J. A., Voltammetric Sensor Array Based on Conducting Polymer-Modified Electrodes for the Discrimination of Liquids. *Electrochimica Acta* **2004,** *49* (26), 4543-4551.
15. Shekarchizadeh, H.; Ensafi, A. A.; Kadivar, M., Selective Determination of Sucrose Based on Electropolymerized Molecularly Imprinted Polymer Modified Multiwall Carbon Nanotubes/Glassy Carbon Electrode. *Mater. Sci. Eng. C Mater. Biol. Appl.* **2013,** *33* (6), 3553-3561.
16. Nayak, J. K.; Parhi, P.; Jha, R., Graphene Oxide Encapsulated Gold Nanoparticle Based Stable Fibre Optic Sucrose Sensor. *Sens. Actuators B Chem.* **2015,** *221*, 835-841.
17. Ahn, J. H.; Seong, T. Y.; Kim, W. M.; Lee, T. S.; Kim, I.; Lee, K. S., Fiber-Optic Waveguide Coupled Surface Plasmon Resonance Sensor. *Opt. Express* **2012,** *20* (19), 21729-21738.

18. Zhang, N. L.; Wei, X.; Fan, Y. X.; Zhou, X. R.; Liu, Y., Recent Advances in Development of Biosensors for Taste-Related Analyses. *Trends Analyt. Chem.* **2020,** *129*, 115925.
19. Ahn, S. R.; An, J. H.; Song, H. S.; Park, J. W.; Lee, S. H.; Kim, J. H.; Jang, J.; Park, T. H., Duplex Bioelectronic Tongue for Sensing Umami and Sweet Tastes Based on Human Taste Receptor Nanovesicles. *ACS Nano* **2016,** *10* (8), 7287-7296.
20. Song, H. S.; Jin, H. J.; Ahn, S. R.; Kim, D.; Lee, S. H.; Kim, U.-k., Bioelectronic Tongue Using Heterodimeric Human Taste Receptor for the Discrimination of Sweeteners with Human-like Performance. *ACS Nano* **2014,** *8* (10), 9781-9789.
21. Ahn, S. R.; An, J. H.; Jang, I. H.; Na, W.; Yang, H.; Cho, K. H.; Lee, S. H.; Song, H. S.; Jang, J.; Park, T. H., High-Performance Bioelectronic Tongue Using Ligand Binding Domain T1R1 VFT for Umami Taste Detection. *Biosens. Bioelectron.* **2018,** *117*, 628-636.
22. Kim, T. H.; Song, H. S.; Jin, H. J.; Lee, S. H.; Namgung, S.; Kim, U. K.; Park, T. H.; Hong, S., "Bioelectronic Super-Taster" Device Based on Taste Receptor-Carbon Nanotube Hybrid Structures. *Lab Chip* **2011,** *11* (13), 2262-2267.
23. Song, H. S.; Kwon, O. S.; Lee, S. H.; Park, S. J.; Kim, U. K.; Jang, J.; Park, T. H., Human Taste Receptor-Functionalized Field Effect Transistor as a Human-like Nanobioelectronic Tongue. *Nano Lett.* **2013,** *13* (1), 172-178.
24. Kwon, O. S.; Song, H. S.; Park, T. H.; Jang, J., Conducting Nanomaterial Sensor Using Natural Receptors. *Chem. Rev.* **2019,** *119* (1), 36-93.
25. Ashikawa, Y.; Ihara, M.; Matsuura, N.; Fukunaga, Y.; Kusakabe, Y.; Yamashita, A., GFP-Based Evaluation System of Recombinant Expression Through the Secretory Pathway in Insect Cells and its Application to the Extracellular Domains of Class C GPCRs. *Protein Sci.* **2011,** *20* (10), 1720-1734.
26. Nuemket, N.; Yasui, N.; Kusakabe, Y.; Nomura, Y.; Atsumi, N.; Akiyama, S.; Nango, E.; Kato, Y.; Kaneko, M. K.; Takagi, J.; Hosotani, M.; Yamashita, A., Structural Basis for Perception of Diverse Chemical Substances by T1r Taste Receptors. *Nat. Commun.* **2017,** *8*, 15530.
27. Bagal-Kestwal, D.; Kestwal, R. M.; Chiang, B. H., Invertase-Nanogold Clusters Decorated Plant Membranes for Fluorescence-Based Sucrose Sensor. *J. Nanobiotechnology* **2015,** *13*, 30.
28. Grembecka, M.; Lebiedzińska, A.; Szefer, P., Simultaneous Separation and Determination of Erythritol, Xylitol, Sorbitol, Mannitol, Maltitol, Fructose, Glucose, Sucrose and Maltose in Food Products by High Performance Liquid Chromatography Coupled to Charged Aerosol Detector. *Microchem. J.* **2014,** *117*, 77-82.
29. Nelson, G.; Hoon, M. A.; Chandrashekar, J.; Zhang, Y.; Ryba, N. J. P.; Zuker, C. S., Mammalian Sweet Taste Receptors. *Cell* **2001,** *106* (3), 381-390.
30. Hoon, M. A.; Adler, E.; Lindemeier, J.; Battey, J. F.; Ryba, N. J. P.; Zuker, C. S., Putative Mammalian Taste Receptors. *Cell* **1999,** *96* (4), 541-551.
31. Xu, H.; Staszewski, L.; Tang, H.; Adler, E.; Zoller, M.; Li, X., Different Functional Roles of T1R Subunits in the Heteromeric Taste Receptors. *Proc. Nat. Acad. Sci.* **2004,** *101* (39), 14258-14263.
32. Kniazeff, J.; Prezeau, L.; Rondard, P.; Pin, J. P.; Goudet, C., Dimers and Beyond: The Functional Puzzles of Class C GPCRs. *Pharmacol. Ther.* **2011,** *130* (1), 9-25.

33. Servant, G.; Tachdjian, C.; Li, X.; Karanewsky, D. S., The Sweet Taste of True Synergy: Positive Allosteric Modulation of the Human Sweet Taste Receptor. *Trends Pharmacol. Sci.* **2011,** *32* (11), 631-636.
34. Fernstrom, J. D.; Munger, S. D.; Sclafani, A.; de Araujo, I. E.; Roberts, A.; Molinary, S., Mechanisms for Sweetness. *J. Nutr.* **2012,** *142* (6), 1134S-1141S.
35. Nango, E.; Akiyama, S.; Maki-Yonekura, S.; Ashikawa, Y.; Kusakabe, Y.; Krayukhina, E.; Maruno, T.; Uchiyama, S.; Nuemket, N.; Yonekura, K.; Shimizu, M.; Atsumi, N.; Yasui, N.; Hikima, T.; Yamamoto, M.; Kobayashi, Y.; Yamashita, A., Taste Substance Binding Elicits Conformational Change of Taste Receptor T1r Heterodimer Extracellular Domains. *Sci. Rep.* **2016,** *6*, 25745.
36. Akbar, S. M.; Sreeramulu, K.; Sharma, H. C., Tryptophan Fluorescence Quenching as a Binding Assay to Monitor Protein Conformation Changes in the Membrane of Intact Mitochondria. *J. Bioenerg. Biomembr.* **2016,** *48* (3), 241-247.
37. Belloir, C.; Savistchenko, J.; Neiers, F.; Taylor, A. J.; McGrane, S.; Briand, L., Biophysical and Functional Characterization of the N-Terminal Domain of the Cat T1R1 Umami Taste Receptor Expressed in Escherichia Coli. *PLoS One* **2017,** *12* (10), e0187051.
38. Jiang, P.; Cui, M.; Zhao, B.; Snyder, L. A.; Benard, L. M.; Osman, R.; Max, M.; Margolskee, R. F., Identification of the Cyclamate Interaction Site Within the Transmembrane Domain of the Human Sweet Taste Receptor Subunit T1R3. *J. Biol. Chem.* **2005,** *280* (40), 34296-34305.
39. Lee, B. Y.; Sung, M. G.; Lee, J.; Baik, K. Y.; Kwon, Y. K.; Lee, M. S.; Hong, S., Universal Parameters for Carbon Nanotube Network-Based Sensors: Can Nanotube Sensors be Reproducible? *ACS Nano* **2011,** *5* (6), 4373-4379.
40. Ishikawa, F. N.; Curreli, M.; Chang, H. K.; Chen, P. C.; Zhang, R.; Cote, R. J.; Thompson, M. E.; Zhou, C., A Calibration Method for Nanowire Biosensors to Suppress Device-to-Device Variation. *ACS Nano* **2009,** *3* (12), 3969-3976.
41. Yeh, P. H.; Li, Z.; Wang, Z. L., Schottky-Gated Probe-Free ZnO Nanowire Biosensor. *Adv. Mater.* **2009,** *21* (48), 4975-4978.
42. Heller, I.; Janssens, A. M.; Mannik, J.; Minot, E. D.; Lemay, S. G.; Dekker, C., Identifying the Mechanism of Biosensing with Carbon Nanotube Transistors. *Nano Lett.* **2008,** *8* (2), 591-595.
43. Toda, Y.; Nakagita, T.; Hayakawa, T.; Okada, S.; Narukawa, M.; Imai, H.; Ishimaru, Y.; Misaka, T., Two Distinct Determinants of Ligand Specificity in T1R1/T1R3 (The Umami Taste Receptor). *J. Biol. Chem.* **2013,** *288* (52), 36863-36877.
44. Masuda, K.; Koizumi, A.; Nakajima, K.; Tanaka, T.; Abe, K.; Misaka, T.; Ishiguro, M., Characterization of the Modes of Binding Between Human Sweet Taste Receptor and Low-Molecular-Weight Sweet Compounds. *PLoS One* **2012,** *7* (4), e35380.
45. Lopez Cascales, J. J.; Oliveira Costa, S. D.; de Groot, B. L.; Walters, D. E., Binding of Glutamate to the Umami Receptor. *Biophys. Chem.* **2010,** *152* (1-3), 139-144.
46. Assadi-Porter, F. M.; Radek, J.; Rao, H.; Tonelli, M., Multimodal Ligand Binding Studies of Human and Mouse G-Coupled Taste Receptors to Correlate Their Species-Specific Sweetness Tasting Properties. *Molecules* **2018,** *23* (10), 2531.
47. Lee, M.; Yang, H.; Kim, D.; Yang, M.; Park, T. H.; Hong, S., Human-like Smelling of a Rose Scent Using an Olfactory Receptor Nanodisc-Based Bioelectronic Nose. *Sci. Rep.* **2018,** *8*, 13945.

48. Yang, H.; Kim, D.; Kim, J.; Moon, D.; Song, H. S.; Lee, M.; Hong, S.; Park, T. H., Nanodisc-Based Bioelectronic Nose Using Olfactory Receptor Produced in Escherichia coli for the Assessment of the Death-Associated Odor Cadaverine. *ACS Nano* **2017,** *11* (12), 11847-11855.
49. Li, X.; Staszewski, L.; Xu, H.; Durick, K.; Zoller, M.; Adler, E., Human Receptors for Sweet and Umami Taste. *Proc. Nat. Acad. Sci.* **2002,** *99* (7), 4692-4696.
50. Waksmonski, J. C.; Koppel, K., Variation in Human Sweet Taste Receptor may Result in Different Levels of Sweet Intensity Variability Between Sweet Stimuli. *Int. J. Food Sci. Tech.* **2016,** *51* (9), 1958-1966.
51. Zhang, F.; Klebansky, B.; Fine, R. M.; Liu, H.; Xu, H.; Servant, G.; Zoller, M.; Tachdjian, C.; Li, X., Molecular Mechanism of the Sweet Taste Enhancers. *Proc. Natl. Acad. Sci.* **2010,** *107* (10), 4752-4757.
52. Hunter, S. R.; Reister, E. J.; Cheon, E.; Mattes, R. D., Low Calorie Sweeteners Differ in Their Physiological Effects in Humans. *Nutrients* **2019,** *11* (11), 2717.
53. Bernhardt, S. J.; Naim, M.; Zehavi, U.; Lindemann, B., Changes in IP3 and Cytosolic Ca2+ in Response to Sugars and Non-Sugar Sweeteners in Transduction of Sweet Taste in the Rat. *J. Physiol.* **1996,** *490 (Pt 2)*, 325-336.
54. Liauchonak, I.; Qorri, B.; Dawoud, F.; Riat, Y.; Szewczuk, M. R., Non-Nutritive Sweeteners and Their Implications on the Development of Metabolic Syndrome. *Nutrients* **2019,** *11* (3), 644.
55. Keast, R. S.; Canty, T. M.; Breslin, P. A., Oral Zinc Sulfate Solutions Inhibit Sweet Taste Perception. *Chem. Senses* **2004,** *29* (6), 513-521.
56. Keast, R. S. J., The Effect of Zinc on Human Taste Perception. *J. Food Sci.* **2003,** *68* (5), 1871-1877.
57. Eisele, T. A.; Drake, S. R., The Partial Compositional Characteristics of Apple Juice from 175 Apple Varieties. *J. Food Compos. Anal.* **2005,** *18* (2-3), 213-221.
58. Finlay, D. B.; Duffull, S. B.; Glass, M., 100 Years of Modelling Ligand-Receptor Binding and Response: A Focus on GPCRs. *Br. J. Pharmacol.* **2020,** *177* (7), 1472-1484.
59. Christine, E. A.; Albert, Y.-K.; Séraphin, K.-C., Determination of the Minerals of the Herbal Tea and Tea Green from Lippia multiflora. *Am. J. Plant Sci.* **2017,** *8* (11), 2608-2621.
60. Ma, X.; Zhao, D.; Li, X.; Meng, L., Chromatographic Method for Determination of the Free Amino Acid Content of Chamomile Flowers. *Pharmacogn. Mag.* **2015,** *11* (41), 176-179.
61. Butt, M. S.; Imran, A.; Sharif, M. K.; Ahmad, R. S.; Xiao, H.; Imran, M.; Rsool, H. A., Black Tea Polyphenols: a Mechanistic Treatise. *Crit. Rev. Food Sci. Nutr.* **2014,** *54* (8), 1002-1011.
62. Jia, X. L.; Ye, J. H.; Wang, H. B.; Li, L.; Wang, F. Q.; Zhang, Q.; Chen, J. B.; Zheng, X. Y.; He, H. B., Characteristic Amino Acids in Tea Leaves as Quality Indicator for the Evaluation of Wuyi Rock Tea in Different Culturing Regions. *J. Appl. Bot. Food Qual.* **2018,** *91*, 187-193.
63. Ekborg-Ott, K. H.; Taylor, A.; Armstrong, D. W., Varietal Differences in the Total and Enantiomeric Composition of Theanine in Tea. *J. Agric. Food Chem.* **1997,** *45* (2), 353-363.
64. Song, H. S.; Jin, H. J.; Ahn, S. R.; Kim, D.; Lee, S. H.; Kim, U. K.; Simons, C. T.; Hong, S.; Park, T. H., Bioelectronic Tongue Using Heterodimeric Human Taste Receptor for the Discrimination of Sweeteners with Human-like Performance. *ACS Nano* **2014,** *8* (10), 9781-9789.

65. Pin, J.-P.; Galvez, T.; Prézeau, L., Evolution, Structure, and Activation Mechanism of Family 3/C G-Protein-Coupled Receptors. *Pharmacol. Ther.* **2003,** *98* (3), 325-354.
66. Oh, J.; Yang, H.; Jeong, G. E.; Moon, D.; Kwon, O. S.; Phyo, S.; Lee, J.; Song, H. S.; Park, T. H.; Jang, J., Ultrasensitive, Selective, and Highly Stable Bioelectronic Nose That Detects the Liquid and Gaseous Cadaverine. *Anal. Chem.* **2019,** *91* (19), 12181-12190.

Table of Contents

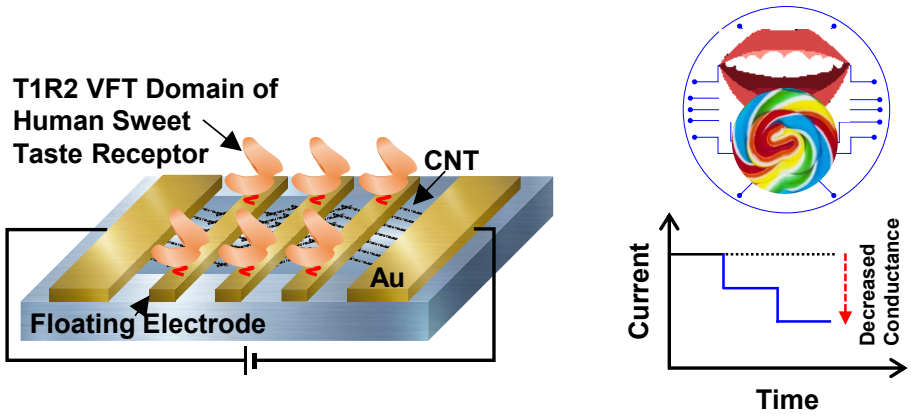

Supporting Information

Ultrasensitive Bioelectronic Tongue Based on Venus Flytrap Domain of Human Sweet Taste Receptor

Jin-Young Jeong[a,†], Yeon Kyung Cha[b,†], Sae Ryun Ahn[c], Junghyun Shin[a], Yoonji Choi[a], Tai Hyun Park[b,d,], and Seunghun Hong[a,*]*

[a]Department of Physics and Astronomy, Seoul National University, Seoul, 08826, Korea

[b]Interdisciplinary Program in Bioengineering, Seoul National University, Seoul, 08826 Korea

[c]Industry Collaboration Center, Industry-Academic Cooperation Foundation, Sookmyung Women's University, Seoul, 04310, Korea

[d]School of Chemical and Biological Engineering, Institute of Chemical Processes, Seoul National University, Seoul, 08826, Korea

[*] To whom correspondence should be addressed.

E-mail: seunghun@snu.ac.kr (S. Hong), thpark@snu.ac.kr (T.H. Park)

Amino Acid Sequence of T1R2 VFT
MAENSDFYLPGDYLLGGLFSLHANMKGIVHLNFLQVPMCKEYEVKVIGYNLMQAMRFAVEE
INNDSSLLPGVLLGYEIVDVCYISNNVQPVLYFLAHEDNLLPIQEDYSNYISRVVAVIGP
DNSESVMTVANFLSLFLLPQITYSAISDELRDKVRFPALLRTTPSADHHIEAMVQLMLHF
RWNWIIVLVSSDTYGRDNGQLLGERVARRDICIAFQETLPTLQPNQNMTSEERQRLVTIV
DKLQQSTARVVVVFSPDLTLYHFFNEVLRQNFTGAVWIASESWAIDPVLHNLTELRHLGT
FLGITIQSVPIPGFSEFREWGPQAGPPPLSRTSQSYTCNQECDNCLNATLSFNTILRLSG
ERVVYSVYSAVYAVAHALHSLLGCDKSTCTKRVVYPWQLLEEIWKVNFTLLDHQIFFDPQ
GDVALHLEIVQWQWDRSQNPFQSVASYYPLQRQLKNIQDISWHTINNTIPM

Table S1. Amino acid sequence of T1R2 VFT.

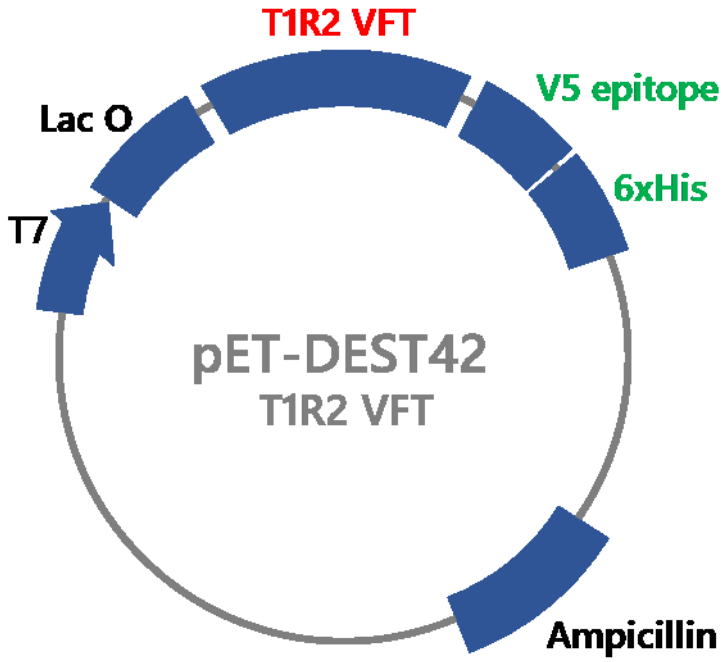

Figure S1. Cloning of T1R2 VFT gene into pET-DEST 42 bacterial expression vector.

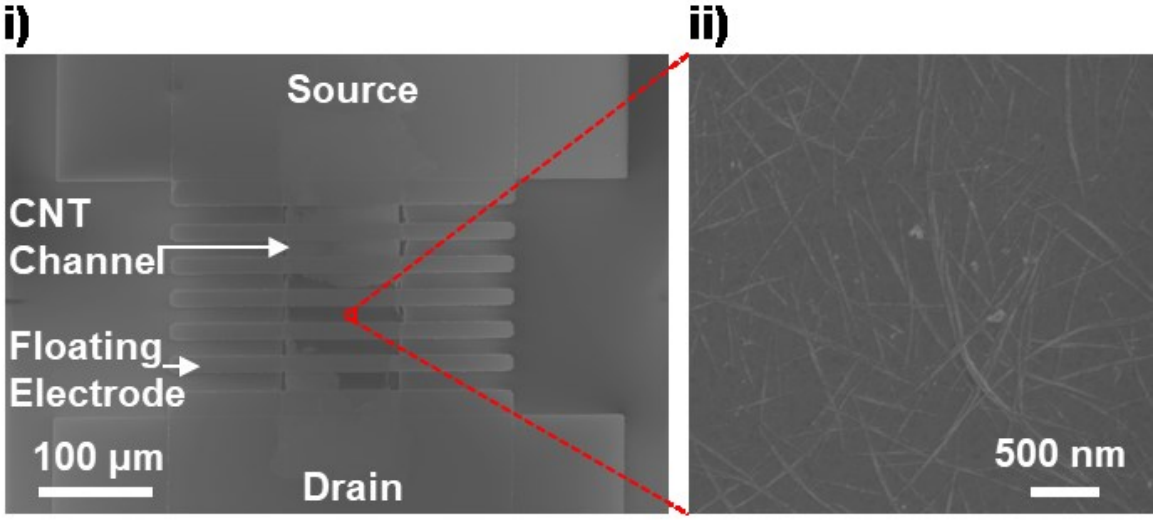

Figure S2. Scanning electron microscope images of (i) the whole channel region and (ii) the CNT channel region of a CNT-FET.

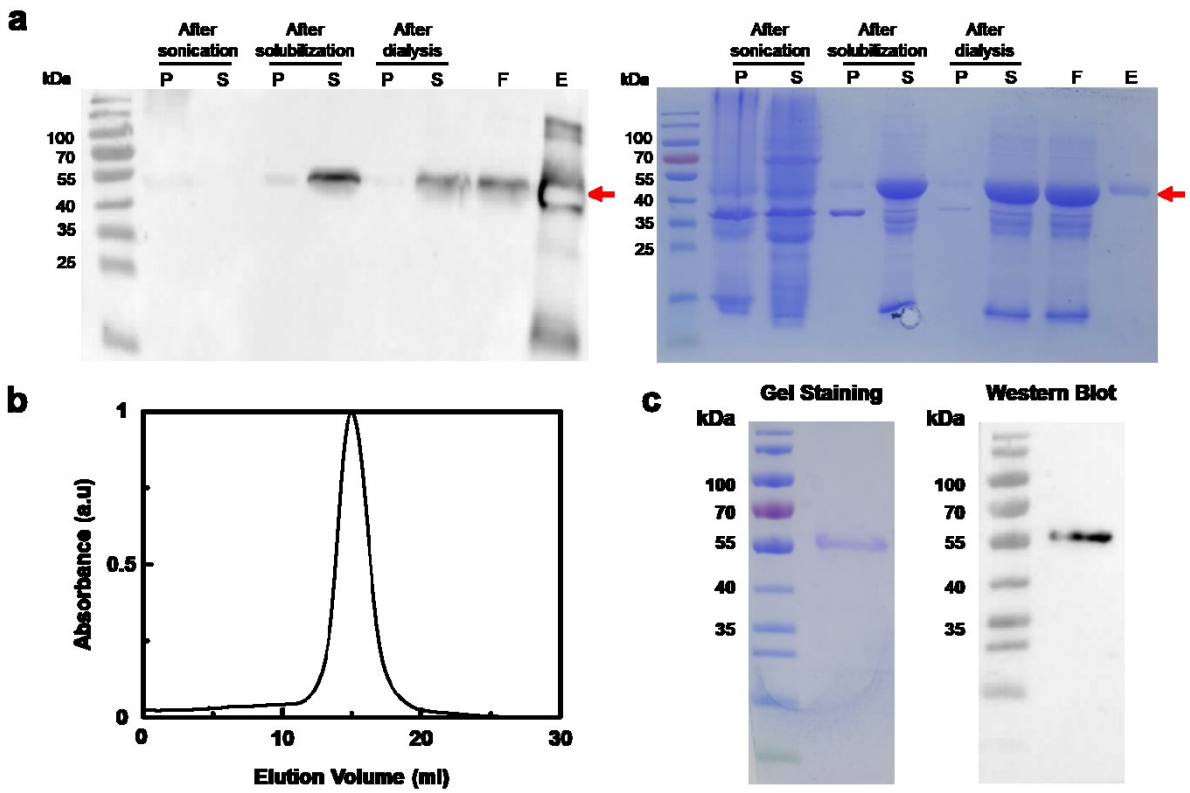

Figure S3. Production of T1R2 VFT in *E. coli.* (a) SDS-PAGE gel staining of T1R2 VFT after cell lysis, solubilization, and purification. P: pellet after centrifugation; S: supernatant after centrifugation; F: filtrate; E: eluent. (b) Fast protein liquid chromatography (FPLC) elution profile of T1R2 VFT. (c) Western blot analysis and SDS-PAGE gel staining of T1R2 VFT after refolding.

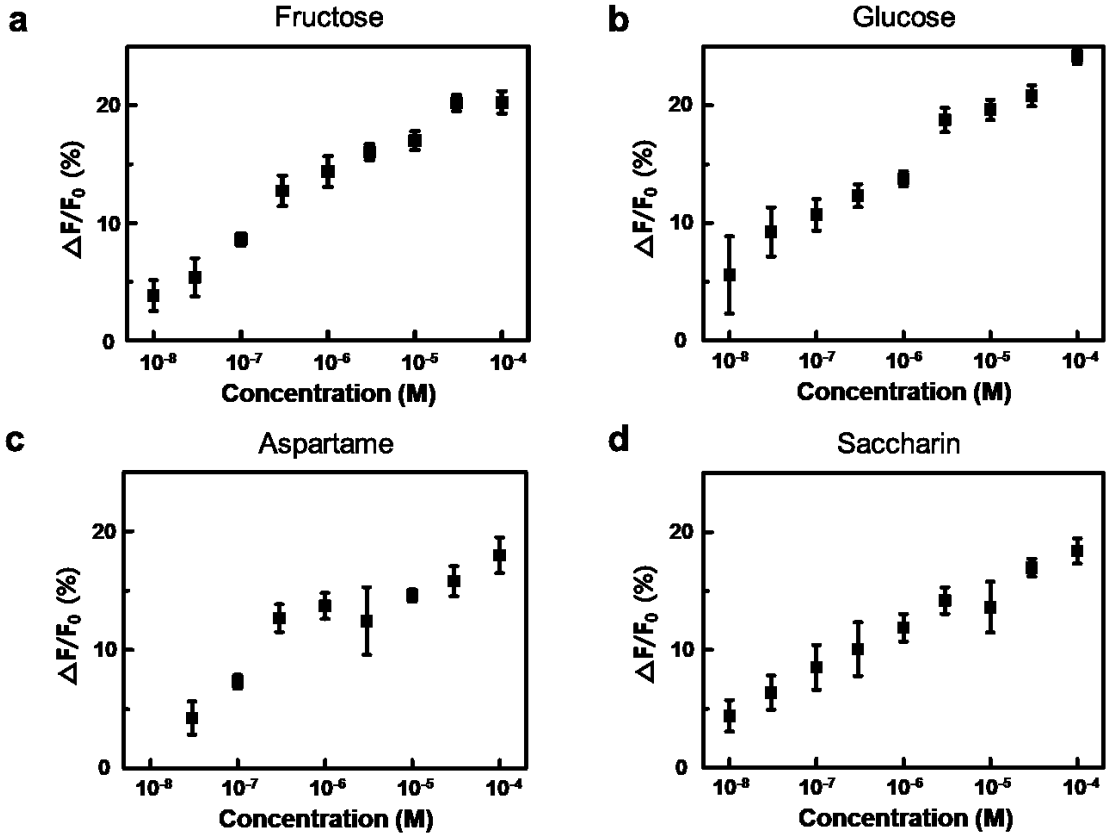

Figure S4. Dose-dependent tests of T1R2 VFT with various sweet taste substances using the tryptophan fluorescence quenching assay. (a) Fructose, (b) Glucose, (c) Aspartame, (d) Saccharin. Data are expressed as means ± standard deviation (n = 5).

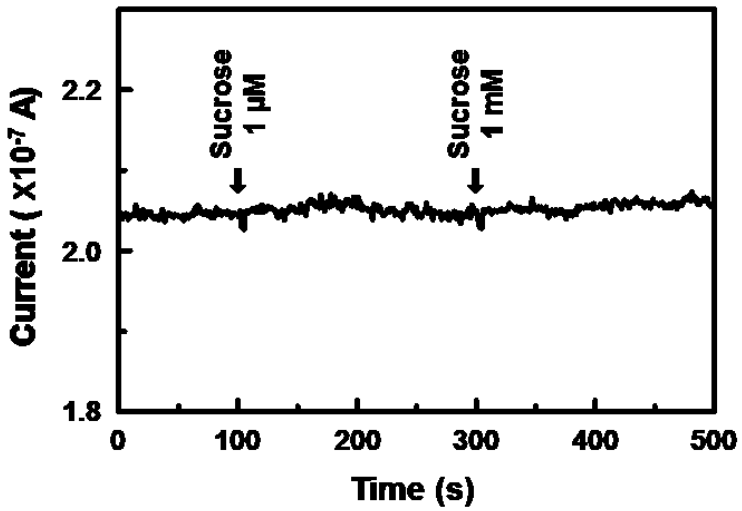

Figure S5. Real-time response of a bare CNT-FET device without T1R2 VFT to sucrose solutions. The device did not respond to the addition of sucrose.

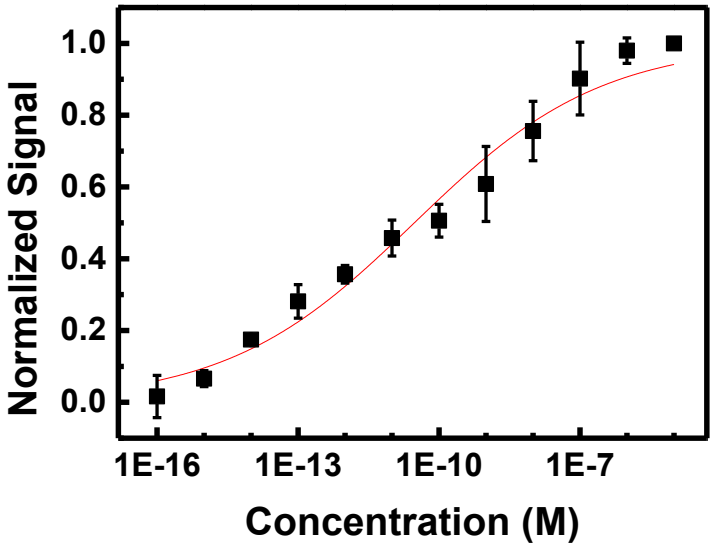

Figure S6. Normalized sensor signals to various concentrations of sucralose (n = 2).

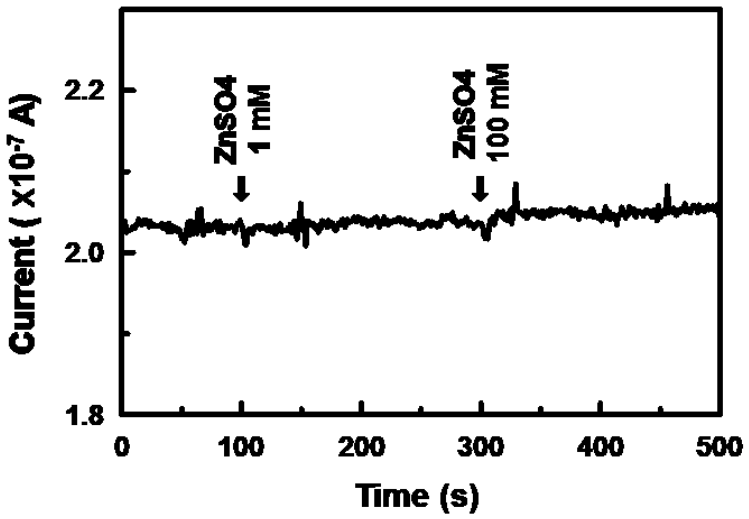

Figure S7. Real-time response of our device to $ZnSO_4$ solutions. The sensor did not respond to the addition of $ZnSO_4$.

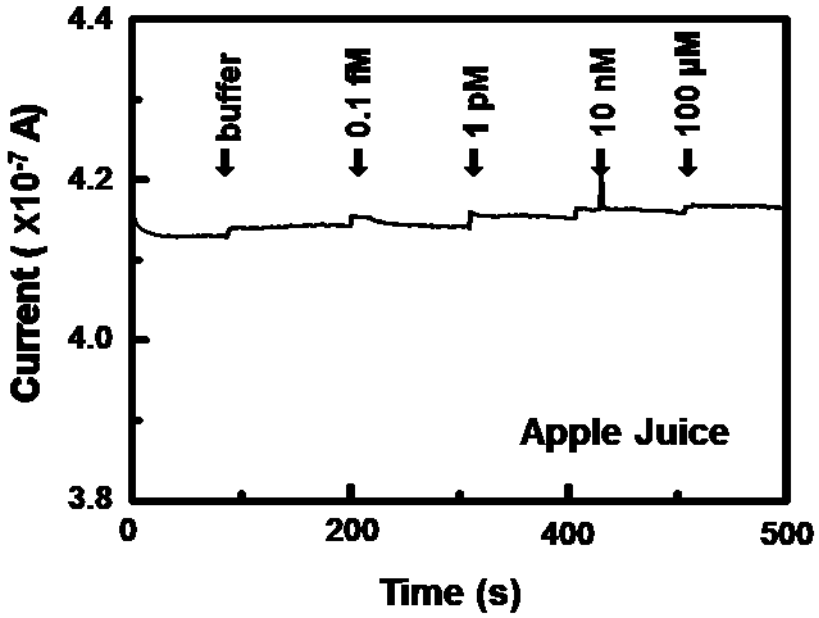

Figure S8. Real-time response of a bare CNT-FET device without T1R2 VFT to apple juice. The device did not respond to the addition of apple juice.

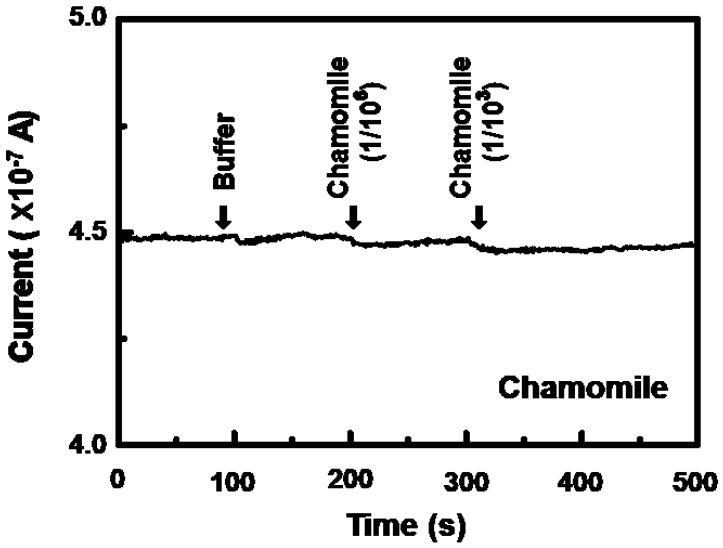

Figure S9. Real-time response of the bioelectronic tongue to the diluted chamomile tea. The device did not exhibit any significant response to the tea without sucrose.

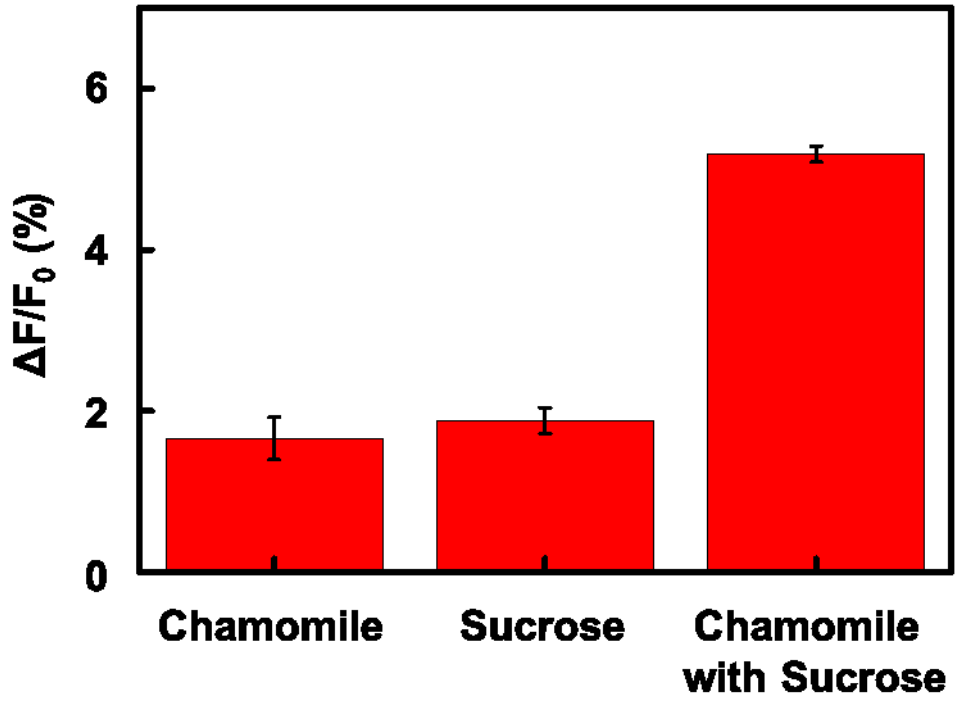

Figure S10. Relative tryptophan fluorescence intensity of T1R2 VFT by the addition of sucrose with or without chamomile tea using the tryptophan fluorescence quenching assay.